Impact of Velocity of Detonation and Charge per Bank Cubic Meters on Flyrock Throw Prediction Using Support Vector Machine

Bright Akuinor Tsidi[1] · Newton Amegbey[1] · Daniel Mireku-Gyimah[1] · Manoj Khandelwal[2]

Abstract

One of the ambient effects of production blasting is flyrock. To effectively manage flyrock throw distance in mining, there is the necessity to successfully envisage blasting output without sacrificing the hazardous impact of flyrock which may result in fatality and operational shutdown. For flyrock throw distance prediction, velocity of detonation (VOD) and charge per bank cubic meter (CPBCM) are not usually included. This paper focuses on the use of support vector machine (SVM) regression to ascertain the impact of VOD and CPBCM on flyrock throw predictions. The machine learning models were linear support vector machine (LSVM), quadratic Gaussian support vector machine (QGSVM), fine Gaussian support vector machine (FGSVM), medium Gaussian support vector machine (MGSVM), and cubic Gaussian support vector machine (CGSVM). The outcome indicates that FGSVM was the most sensitive with a 4% improvement when VOD and CPBCM were included. As a result, the LSVM model provides a suitable AI competitive alternative tool for flyrock throw prediction in mining operations by incorporating VOD and CPBCM.

Keywords Blasting · Flyrock · SVM · Machine learning · VOD

1 Introduction

When explosives are detonated during rock blasting, some rocks are forcefully expelled to distant locations from the blasting area, commonly known as flyrock. The distance that these flyrock fragments travel depends on various factors associated with rock excavation, some of which can be controlled while others cannot. The controllable parameters that have an influence on predicting flyrock include factors such as the depth of the blast hole, powder factor (explosive charge per unit volume of rock), spacing between blast holes, burden (distance between blast hole and rock face), diameter of the blast hole, stemming (material used to plug the blast hole), type of explosive material used, and subdrilling (depth of additional drilling). On the other hand, uncontrollable parameters that are beyond the control of the

blast engineer include rock properties, such as compressive strength, joint spacing, and tensile strength [1, 2]. These uncontrollable parameters play a significant role but cannot be directly manipulated. Several empirical equations have been proposed to simulate the occurrence of flyrock, which is expected to happen as a result of the blasting operation [1–4]. Furthermore, rock mass characteristics exhibit a significant role in the fragmented rock upheaval throughout blasting [5]. The rock density and some rock mass characteristics have virtually been overlooked in all the empirical models [5, 6]. Amini et al. [7] also conducted research to predict flyrock throw using a support vector machine (SVM) and the following input parameters powder factor (PF), hole length (HL), subdrill (SD), spacing (S), hole diameter (D), burden (B), and stemming length (ST) without considering the velocity of detonation (VOD) and charge per bank cubic meter (CPBCM).

As the explosive moves through the explosive column, its potency is taken into consideration by the VOD. The cost component per bank cubic meter of blast undertaking is taken into account by the CPBCM. The VOD of explosives and CPBCM are not usually considered in the flyrock throw distance prediction. Combining the rarely used input parameter and structural risk minimization (SRM) of SVMs seems

✉ Manoj Khandelwal
  m.khandelwal@federation.edu.au;
  mkhandelwal1@gmail.com

1 Mining Engineering Department, University of Mines and Technology, Tarkwa, Ghana

2 Institute of Innovation, Science and Sustainability, Federation University Australia, Ballarat, VIC 3350, Australia

novel because it incorporates the concept of finding an upper limit on the generalization error [8]. SVM also deals with a convex quadratic optimization problem, which means it uses the Karush–Kuhn–Tucker (KKT) principles to find the global optimum. This explains why SVM outperforms other algorithms in so many fields [8].

This paper, therefore, seeks to explore the predictive capability of SVM with input parameters such as cost charged per bank cubic meter (CPBCM) and velocity of detonation (VOD), along with traditional geometric parameters of fragmentation and flyrock throw distance. The effectiveness of SVM for predicting flyrock throw distance will help attain innovation and infrastructure protection as well as sustainable cities and communities.

1.1 Overview of Flyrock Throw Distance

Currently, among the recent efficient tools for predicting these flyrock outcomes were hybrid dimensional analysis fuzzy inference system (H-DAFIS), artificial neural network (ANN), biogeography-based optimization (BBO), gene expression programming (GEP), multiple linear regression (MLR), support vector machine (SVM), fuzzy interface system (FIS), fuzzy rock engineering system (FRES), and extreme learning machine (ELM) [1, 9–12]. Table 1 shows the previous works on AI techniques for fragmentation and flyrock throw distance predictions.

Raina et al. [33] determined the pressure-time record of blasts by exploiting a pressure probe, which has been verified and proven. On the other hand, because of these simplifications, the technique proposed pressure probe has proven to be a more efficient method for predicting flyrock distance. Using this method, which gauges pressure-time data, the flyrock distance and blast danger zone can be estimated around mines that carry out blasting operations [33]. The rock mass itself responds to dynamic fracturing via the processes of dynamically moving cracks and crack growth under dynamic loading conditions. Tests are limited in number, but they are used to determine whether flyrock is present and to find out how much pressure is involved. While the aforementioned tests are quite advanced and are meant to demonstrate a single bench with similar lithology, they are still useful in conveying the basics of mineral testing. Not only does this experiment cost a lot, but it is impossible to implement on a large scale for flyrocks, because pressure probes are too expensive [33].

Table 1 Previous works on AI techniques for fragmentation and flyrock throw distance predictions (modified after [13–15])

References	Method	Inputs	Dataset	R^2
[15]	ANN	B, GSI, S, HL, SD, ST, W/N, PF	200	0.93
[16]	SVM	HL, S, B, SD, ST, PF	187	0.95
[17]	ANN	HD, RD, S, B, ST, PF, SD, N, C	250	0.98
[18]	ANN	B, D, C, HD, S	310	0.98
[19]	GA-ANN	SD, PF, HD, B, S, ST, RMR, D, C	195	0.89
[20]	AHP-TOPSIS, MADM	ST, C, SD, HD, PF, BS, D, B	192	0.98
[21]	ANN, SVM	SD, S, D, B, ST PF, HL	245	0.92, 0.97
[22]	PSO-ANN	HD, SD, S, N, ST, PF, B, RD, C, D	44	0.94
[23]	ANFIS, ANN	BS, C, PF, ST	166	0.83, 0.98
[24]	ANFIS-ANN	PF, C	232	0.92, 0.98
[25]	ANN-PSO	S, N, J, B, ST, D, L, C, PF, RD	44	0.93
[26]	ANN	N, C, SD, B, S, RD, HD, ST, PF	250	0.98
[27]	FIS	S, B, HD, SD, PF, RD, ST, C	490	0.98
[28]	ANN	C, RD, N, B/S, HD, ST, PF, SD	39	0.97
[29]	FIS, ANN	S, HL, ST, B, PF, Q	230	0.96, 0.94
[30]	ICA-ANN	PF, BS, ST, C, Rn, HD, RD,	113	0.83
[31]	ANN	q_l q B, ST, σ_c RQD	95	0.98
[32]	ANN-ACO	B, S, T, H, PF	97	0.94

D hole diameter, *B* burden, *S* spacing, *HD* hole depth, *Sd* Subdrill, *PF* powder factor, *ST* stemming, *H bench height, VOD* velocity of detonation, *Q* explosive charge, *BI* blastability index, *RMR* rock mass rating, q_l *linear concentration of charges*, *q specific charge*, σ_c *unconfined compressive strength*, J Joint density, R_n Schmidt hammer rebound number, SD specific drilling, RD rock density, N number of rows, W/N charge in each delay, *MC* maximum charge per delay, *CPD* charge per delay, *ICA* imperialist competitive algorithm, *ANN* artificial neural network, *SVR/M* support vector machine/regression, *FIS* fuzzy inference system, *PSO* particle swarm optimization, *RQD* rock quality designation, GSI Geological strength index, *GA-ANN* genetic algorithm, *MLR* multiple linear regression, ANFIS Adaptive Neuro-Fuzzy Inference System, TOPSIS Technique for Order of Preference by Similarity to Ideal Solution, MADM Multi-attribute decision making, *ACO* ant colony optimization

Additionally, Sawmliana et al. [34] tried to replicate the effect of a similar blast in the mines that caused the flyrock incident. A digital video camera was used to record all the blasting trials. Based on the replicated results, the burden relief success rate was at least 80% with adequate delay recesses for the blasted rock movement. If various flight rock prediction models are employed, the maximum possible traveling distance for flinging fragments is 227 m. It was observed that the only upward throws of the flyrock happened to be from about 70 m in elevation in the trial explosion. Since it was hard to discover the actual cause of the flyrock outbreak, it must have been difficult to infer. However, Sawmliana et al. [34] after their extensive investigation concluded that it is highly possible that the source of flying rocks traveling a distance of 280 m could be a weak zone in the rock strata.

Along this line of reasoning, Hasanipanah et al. [35] researched the Ulu Tiram Quarry in Malaysia where risk assessment and the prediction of flyrock were envisaged. It was realized that in order to tackle the first objective of risk associated with flyrock, the fuzzy rock engineering system (FRES) framework needs to be applied. The proposed FRES thoroughly tested parameters that influence flyrock, which can help determine future decisions when situations are ambiguous because of its ability to handle multiple inputs and scenarios. Flyrock's risk was evaluated with 11 different parameters, and the proposed FRES could take into account

these interactions. The parameters are burden (B), powder factor (PF), hole depth to burden ratio (H/B), spacing to burden ratio (S/B), maximum charge per delay (MC), stemming and burden ratio (St/B), burden, diameter ratio (B/D), blastability index (BI), rock mass rating (RMR), and hole diameter (D) and VOD parameters. The most sensitive parameters on the cause-and-effect diagram ($C + E$ or $C − E$) were PF, B, and H/B, which possess the highest values of $C + E$ (interactive intensity). The RMR, with the maximum $C − E$, is the dominant system factor, and the system factor with the lowest $C − E$ is the MC. Based on the findings, flyrock risk was found to be moderate to high at Ulu Tiram Quarry. Thus, it was recommended that using a controlled blasting method at Ulu Tiram Quarry is of the essence. Genetic algorithm (GA) was also employed to simulate flyrock, and it was discovered that the GA-based algorithm provided more precise predictions than the particle swam optimization (PSO) and imperialist competitive algorithm (ICA) constructed models.

From the works of previous authors, the most common parameters for flyrock throw prediction are explosives specific gravity (SGe), hole diameter (D), burden (B), spacing (S), hole depth (HD), subdrill (SD), powder factor (PF), stemming (ST), and explosive charge (Q). A review of the various AI techniques, their authors, the input used, the total datasets, and the coefficient of determination achieved for flyrock throw prediction is illustrated in Table 1.

Fig. 1 Location of gold fields Ghana Damang mine [36]
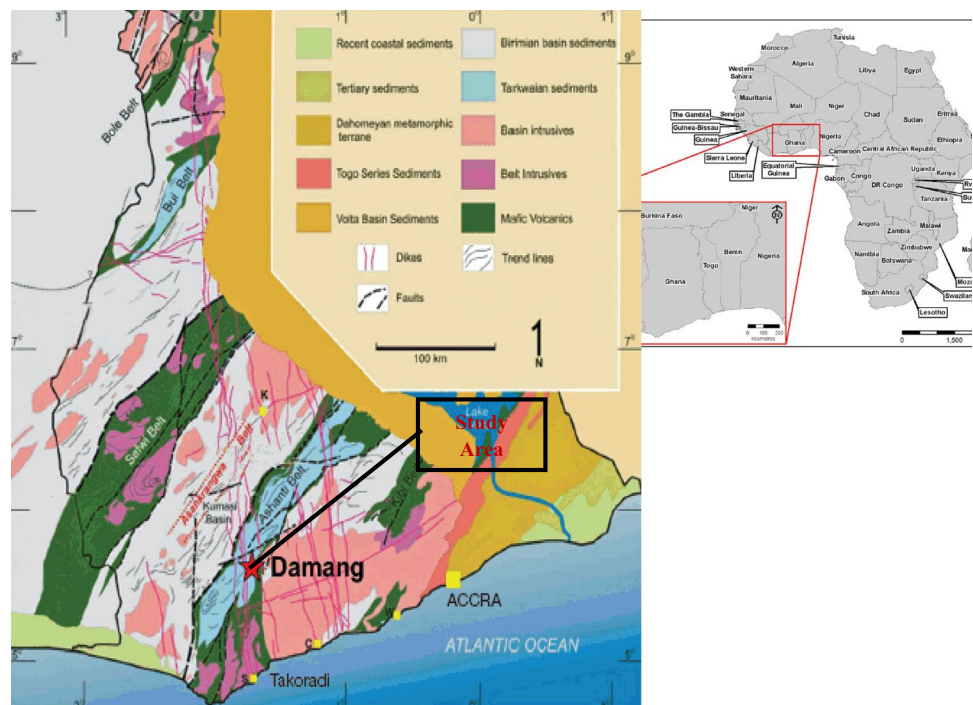
2 Materials and Methods

Gold Fields Ghana Limited Damang (GFGLD) mine is located in the southwestern part of Ghana, which is approximately 300 km away from the capital, Accra, by road. GFGLD mine is located at a latitude of 5° 11′ N and longitude of 1° 57′ W [36–38] (Fig. 1). To the north of and connected to the Tarkwa concession is the Damang commercial enterprise, which is found near the town.

2.1 Data Collection

Data was collected for drill and blast parameters and was used to predict flyrock. The whole data set was 2629. The input parameters were summarized in Table 2: explosives specific gravity, hole diameter, burden, spacing, hole depth, subdrill, powder factor, rate charged per bank cubic meter, stemming, velocity of detonation, VOD, and explosive charge while the output was flyrock. This secondary data was collected over 2 years spanning April 2018 to March 2020.

The dataset was analyzed in Matrix Laboratory (MATLAB) software, and the corresponding results are also indicated in Table 2. The collected data also included the geological condition of the operating mine (see Fig. 2).

Figure 2 shows the description of the rock formation as good rock mass with a rating between 70 and 90 (color coded as green), fair rock mass with a rating of 50–70 (color coded yellow), poor rock mass with a rating of between 25 and 50 (color coded brown), and very poor rock mass with a rating of less than 25 (color coded red). The following drill patterns used for the various domains are designated as follows 3.5 m by 3.5 m for (phyllites and diorites), 3.7 m by 4.3 m (all waste zones), and 3.8 m by 3.8 m (huni sandstones) all at depths of 9 m and 6 m as and when needed.

The modeling was carried out using machine learning models in MATLAB and using a Hewlett-Packard (HP) laptop with Intel® Core™ i7. The predictive accuracy of the various spawns of SVM was discovered, and the best-performing posteriors were selected.

2.2 Methods

Over the years, a series of empirical methods have been developed and used by several researchers [1, 5, 6, 39–44]. It was realized that the predictive performance of empirical models always trails behind AI models [6]. Among the AI techniques are support vector machines (SVM). SVM has proven its robustness in the field of engineering predictions. The standard SVM and least square support vector machines were examined to test their predictive capability using large datasets and input parameters seldom used for flyrock throw distance prediction.
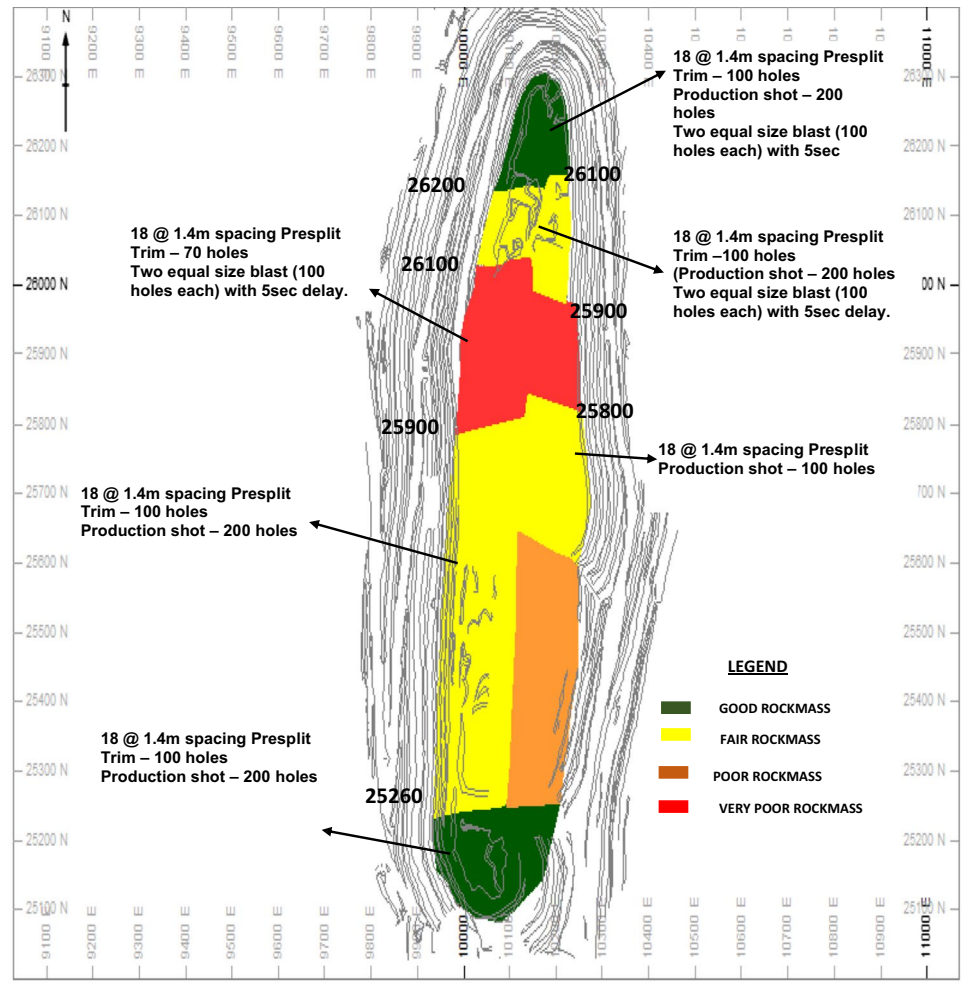
2.3 Support Vector Machine

A support vector machine (SVM) is a sparse technique, like all other nonparametric methods [45]. SVM is a sorting technique built on arithmetical knowledge and the Vapnik–Chervonenkis (VC) dimensional models [46]. The SVM is a set of interrelated controlled learning methods that process data and extricate patterns. It is used for classification and regression studies [47]. In contrast to a neural network, which achieves only a local minimum, SVR introduces a global optimization by applying a methodology that eliminates structural risk [48]. The rudimentary code is fleetingly presented as, for any given sample sets (x_i, y_i), $1 \leq i \leq T_n$ as training samples, where T_n is the entire number of vectors. Training vectors $x_i \in (R_n)$ are the random number/(contribution vectors), and D_x is the dimension of the input space. y_i denotes the corresponding yield of x_i, $y_i = \pm 1$, which is designated as precipitation occurrence or not here.

Table 2 Input parameters

Parameter	Symbol	Maximum	Minimum	Average	Average deviation	Standard deviation
Subdrill (m)	SD	1.20	0.30	0.93	0.19	0.21
Explosive gravity	Sg	165.00	115.00	123.24	6.99	9.84
Hole depth (m)	HD	18.00	3.00	6.97	1.48	1.65
Stemming length (m)	St	4.13	0.00	2.99	0.26	0.36
Hole diameter (mm)	D	165.00	115.00	123.24	6.99	9.84
Powder factor (kg/m³)	PF	1.90	0.28	0.71	0.45	0.31
Spacing (m)	S	5.00	2.50	3.87	0.25	0.34
Burden (m)	B	5.00	2.50	3.72	0.29	0.36
Explosive charge (kg)	Q	370.76	46.26	70.11	27.53	31.28
Velocity of detonation (m/s)	VOD	4000.00	2900.00	3443.12	279.29	322.34
Cost per bank cubic meter ($/BCM)	CPBCM	2.70	0.15	1.68	0.18	0.25

Fig. 2 Pit lithology domains using rock mass rating (RMR)

2.3.1 Variants of Support Vector Machine

The parting hyperplane is represented as $\Psi^* x + \gamma = 0$, where (*) is the inner product. w is the weight vector, and b represents the bias term [49]. Equation (1) represents the classification hyperplane. Any of the training samples that fall on the hyperplane form the equal sign of Eq. (1), called the support vector

$$(\Psi^* x + \gamma) \geq 0 \tag{1}$$

For better optimization of the range or to take full advantage of the range, one only needs to maximize $\| \Psi \|^{-1}$, which is equivalent to minimizing $\frac{1}{2}\| \Psi \|^2$. The rudimentary kind of SVM is as revealed in expression (2):

2.3.2 Least Squares Support Vector Machines

The least squares support vector machine (LS-SVM) was spearheaded by An et al. [50]. Furthermore, these techniques have been efficaciously applied to numerous global areas

of research. Finally, while the less popular LS-SVM is not quite as widely used as the standard SVM, in a broad range of benchmark information sets, LS-SVM and standard SVM accomplish about the same. A hyperparameter (i.e., kernel parameter or regularization parameter) is used in the design of LS-SVM models.

$$\text{Min} \left[\frac{1}{2}\|\Psi\|^2 \right] \tag{2}$$

subject to $y_i (\Psi^* x + \gamma) - 1 \geq 0$, where $i = 1, 2, \cdots, T_n$ with reference to Eq. (2), a hyperplane can be obtained as $w \cdot x_i + b = 0$ with the largest margin. Considering the equality constraints in Eq. (2), they can be unconstrained by applying the Lagrangian relation, and this is done by introducing the soft margin, to make a soft margin adapt to noisy data if the case is undivided, leading to Eq. (3):

$$\text{Min} \left[\frac{1}{2}\|\Psi\|^2 \right] - C \sum_{i=1}^{T_n} l_o \left[y_i (\Psi * x + \gamma) - 1 \right] \tag{3}$$

$l_{0/1}$ is the 0/1 loss function.

C is a constant bigger than 0, and when C is infinite, the imposition of the constraint that all samples meet the requirements is engaged. Otherwise, a room is created for samples that do not meet the requirements to be used. The two main problems here are the maximization of the objective function and the writing of a quadratic program, both of which must be addressed to solve the problem. If an equation is solvable, then Eq. (4) is arrived at

$$\max_{\alpha} \sum_{i=1}^{T_n} \alpha - \frac{1}{2} \sum_{i=1}^{T_n} \sum_{j=1}^{T_n} y_i y_j \alpha_i \alpha_j (x_i y_j) \tag{4}$$

$$\sum_{i=1}^{T_n} \alpha_i y_i = 0$$

Subject to

$$0 \leq \alpha \leq C$$

$$i = 1, 2, \ldots \ldots T_n$$

Vapnik [51] and Du et al. [49] described this as an extremum tricky problem of a quadratic function having inequality variables that present a unique solution. A_i is a Lagrange multiplier for each training sample, and the sample is the support vector for which a_i in Eq. (4) = 0, overlay on one of the two hyperplanes:

$$(\Psi^* x) + \gamma = +1; \tag{5}$$

$$(\Psi^* x) + \gamma = -1 \tag{6}$$

The code of the Karush–Kuhn–Tucker (KKT) state indicates that the optimization problem requirement needs to satisfy Eqs. (5) and (6) when dealing with the nonlinear SVM problem. The SVM presents a kernel function to enable easy plotting of the data and transforms the data into a high-dimensional space [49, 51]:

$$\max_{\alpha} \sum_{i=1}^{T_n} \alpha - \frac{1}{2} \sum_{i=1}^{T_n} \sum_{j=1}^{T_n} y_i y_j \alpha_i \alpha_j \text{KKT}(x_i x_j) \tag{7}$$

where the KKT(x_i, x_j) is the kernel function, KKT(x_i, x_j) = $\phi(x_i) \cdot \phi(x_j)$.

Once the training algorithm gives the expression $\phi(x_i) \cdot \phi(x_j)$, we can use the $K(x_i, x_j)$ in its place.

The parameter is identical to Eq. (7), and $0 \leq \alpha_i \leq C$. SVM is grounded upon the learning of the kernel. The kernel function is a crucial component of the algorithm. When choosing a kernel function, a crucial location needs to be selected, and this has a direct impact on the model's generalization capabilities [46]. Many kernel functions, including the RBF function, are used often (8). An ace, simple, and easy-to-use kernel function that helps the RBF's nonlinearity issues is the RBF radial basis function (RBF RBF) [50].

2.3.3 Gaussian Support Vector Machine

Until now, the only functions used by the kernel are as follows: fractional Brownian motion, kernel polynomial, kernel function, and sigmoid kernel [52]. No matter the situation in low-dimensional cases or in high-dimensional cases, small sample numbers, or significant sample numbers, the Gaussian kernel function is applied in all three of these kernel functions, a broader area of convergence for the Gaussian kernel and a better classification. According to the fundamental theorem of inner products, which asserts that inner products are essentially equivalent to feature space, the kernel function is well defined as the inner products of feature space. In essence, dot products are interpreted as how closely two features are located to each other in feature space. The level of similar degree differs in positive proportion to the worth of $K(x_i, x)$. In model space, Euclidean distance $d(x,y)$ $Z(x_i - y_i)2$ ($i = 1, 2, ..., n$) is frequently used to define the similarity in degree between sample x and y, where n is the dimension of sample in Eq. (8) [53].

$$K(x_i x_j) = \exp \{-g P x_j - x_i P^2\} \tag{8}$$

where g represents the kernel constraint to quantify the breadth of the kernel function in RBF.

Suppose unfitting occurs with g, the results of the process may outfit or overfit the training data. This function is vigorous and can account for the nonlinear decision border [49].

The Gaussian kernel is based on the notion that similar points in the feature space are close to each other and only depend on the Euclidean distance between x and x_i (in terms of Euclidean distance). In many circumstances, this assumption is fair; hence, the Gaussian kernel is frequently utilized in practice. For a Gaussian kernel: $K(x, x_i) := e^{-g\|x-x_i\|^2}$ (for a given parameter $\gamma > 0$) it works well [53].

A new constraint is enforced on the optimization problem: the hyperplane must be located far away from the classes. We use the term Gaussian kernel because it services the optimization phase to discover the hyperplane that is situated at the greatest distance from the classes while still being equidistant from them. Training needs to take place on a subset of the overall population. Prediction, on the other hand, requires making predictions on things that have not yet occurred [45].

Awad and Khanna [45] stated that structural risk minimization (SRM) is used in conjunction with structural optimization minimization (SOM) to obtain the two solutions and convexity requirements. The SRM is an inductive code that, from a finite training dataset, selects a learning model. The SRM model suggests a trade-off between the VC extents, which is to say the space required, and the deviation of empirical measurements. In convex optimization, with
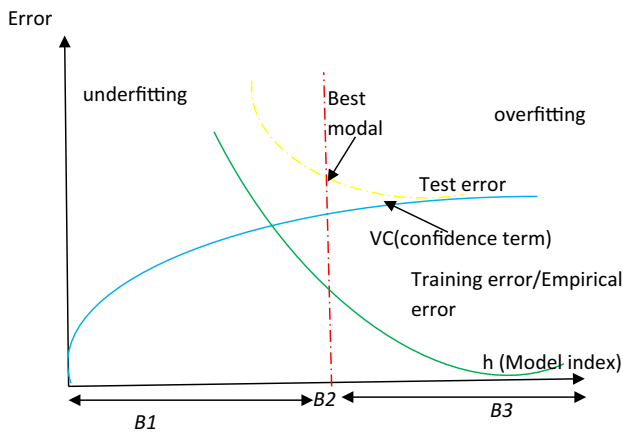
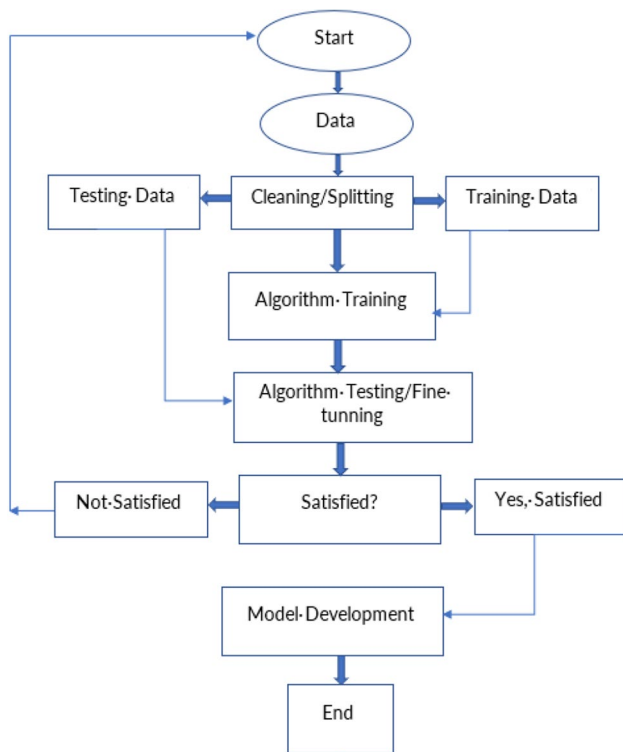**Fig. 3** Connection between error trends and model index

Fig. 4 Flow chart of modeling

m constraints and *n* variables to be maximized, SRM has developed a novel method to solve the problem in polynomial time. The SRM sequenced models are placed in order of increasing complexity [45]. Figure 3 shows the complete model error variation with the involvedness index of any machine learning model.

Figure 3 illustrates complex models, as evidenced by the elevated error at (B1). Since a basic model does not describe entirely the complexity of the data, a model underfitting the data occurs, which results in a high error and a maximum

error (B3). (B3) is overfitting, as described in Fig. 3, and occurs in the early stages of training when the structure begins adapting its learning model to the training data, resulting in overfitting that reduces the training error value while simultaneously increasing the model validation coefficient. B2 has the least amount of error; hence, the best result is obtained at the intersection of the B2 and the test error. When this is achieved, then the best model is ready to be implemented [54].

During the modeling of support vector machines for flyrock throw distance prediction, the procedures undertaken are illustrated in Fig. 4. The process started with the collection of raw secondary data. After the data collection, data processing was carried out by cleaning data and splitting data. The processed data then goes through the SVM model for training, fine-tuning, validation, and testing. If the desired result of prediction was obtained, then the process was truncated, if not, the whole process was repeated.

The empirical equations for flyrock throw prediction are as follows:

Chiapetta (1983) proposed Eqs. (9) to (11) for the distance traveled by the rock from the blast horizontally, the initial velocity of the flyrock at an angle, and the size of the projectile flyrock respectively [41].

$$FR_1 = V_O \left(\frac{2 \sin 2\theta}{g} \right) \tag{9}$$

$$V_O = \left(\frac{10D(2600)}{T_b \times \rho_r} \right) \tag{10}$$

$$T_b = 0.1 \left(D^{\frac{2}{3}} \right) \tag{11}$$

where

FR_1 is the distance traveled (m) by the rock along a horizontal line at the original elevation of the rock on the face,

V_0 is the initial velocity of the flyrock and θ is the angle of departure with the horizontal,

g is the gravitational constant,

d is hole diameter in inches,

T_b is the size of rock fragment (m), and

ρ_r is the density of rock in g/cm^3.

An empirical model was established by Lundborg et al. (1975) based on hole and rock diameters as follows [43]:

$$\text{FR}_m = 260\left(\frac{D}{25}\right)^{\frac{2}{3}} \tag{12}$$

$$T_b = 0.1(D)^{\frac{2}{3}} \tag{13}$$

where

FR_m is the maximum rock projection in meters,

D is the hole diameter in inches, and

T_b is the size of rock fragments in meters.

Gupta (1980) suggested an empirical equation to predict flyrock distance based on stemming length and burden [44].

$$L = 155.2(d)^{-1.37} \tag{14}$$

$$\text{FR} = \left(\frac{155.2}{L}\right)^{1/_{1.37}} \tag{15}$$

where

L is the ratio of stemming length to burden and

FR is the distance traveled by the rocks in meters.

According to McKenzie (2018), the minimum stemming length can be estimated using Eqs. (16) to (18) [55].

$$St_{\min} = 0.03 \times \frac{\left(m \times \rho_e\right)^{0.333} \times D^{1.31}}{\left(\frac{\text{Range}_{\max}}{\text{FoS}}\right)} - 0.0005 \times m \times D \tag{16}$$

Flyrock range with a safety factor of 1 is given as:

$$\text{FR} = \frac{\left(m \times \rho_e\right)^{0.333} \times D^{1.31}}{St - 0.0005 \times m \times D} \tag{17}$$

Scaled depth of burial (SDOB)

$$\text{SDOB} = \frac{St + 0.0005 \times m \times D}{0.00923 \times \left(m \times D \times \rho_e\right)^{0.333}} \tag{18}$$

where

St   is the stemming length,

m is the explosive charge length,

D is the blast hole diameter,

$\boldsymbol{\rho}_e$ is the explosive density,

FoS   is the factor of safety, and

$\text{Range}_{\text{Max}}$ is the maximum flyrock range.

3 Results and Discussion

The study and analysis clearly demonstrate the significant role of artificial intelligence in blasting operations and their environmental consequences. In light of this, the utilization of support vector machines (SVMs), which is one form of AI, was investigated.

In order to develop effective models, various types of SVMs were examined, including linear, quadratic, cubic, fine Gaussian, medium Gaussian, and coarse Gaussian. For all these models, automatic kernel functions and kernel scales were employed. The fine Gaussian, medium Gaussian, and coarse Gaussian SVMs utilized optimal kernel scales of 0.79,

Table 4 Testing results

SVM model (testing with VOD and CPBCM)	R^2	RMSE
MGSVM	0.96	0.33
CGSVM	0.99	0.35
QGSVM	1.00	0.13
LSVM	1.00	0.05
FGSVM	0.51	1.06

Table 3 Training results

SVM model (testing without VOD and CPBCM)	R^2	RMSE
MGSVM	0.82	1.32
CGSVM	0.96	0.65
QGSVM	0.99	6.50
LSVM	1.00	0.25
FGSVM	0.40	5.75

Table 5 Impact of VOD and CPBCM on overall results

AI techniques	R^2%	RMSE%
MGSVM	14.00	75.00
CGSVM	3.00	65.00
QGSVM	1.00	98.00
LSVM	0.00	80.00
FGSVM	39.5	94.00

a

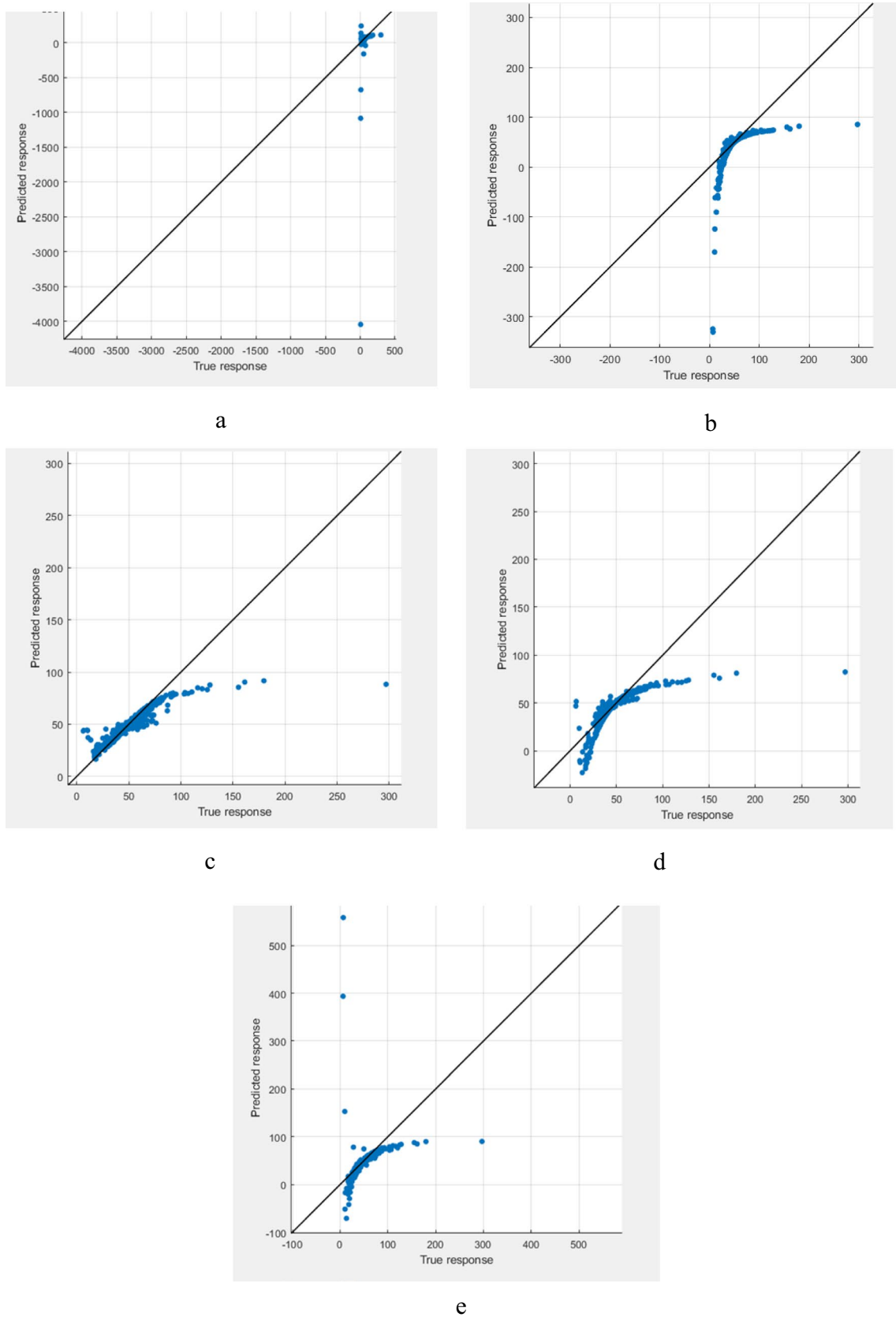b

c

d

e

Fig. 5 **a–e** Parity plots for the SVM models

Table 6 Comparisons of statistics of empirical models

	Chiapetta (1983)	Gupta (1980)	McKenzie (2018)	Lundborg et al. (1975)
R^2	0.87	0.82	0.92	0.69
RMSE	142.18	94.07	65.92	38.40

3.2, and 13, respectively. The training and testing times ranged from 3.66 s for the fine Gaussian SVM to a maximum of 104.24 s for the coarse Gaussian SVM. The number of observations processed per second varied from 62,000 observations for the medium Gaussian SVM to 150,000 observations for the linear Gaussian SVM. Throughout the analysis, automatic box constant, epsilon, and standardization were enabled for all SVMs. The outcomes of this analysis are presented in Tables 3 and 4, respectively.

Following this analysis, an investigation was conducted to determine the influence of the velocity of detonation (VOD) of the explosive and the charge per bank cubic meter (CPBCM) of the blasted material on the model development. Please refer to Table 5 for the results of this investigation.

According to the data presented in Table 3, it is evident that the fine Gaussian SVM (FGSVM) exhibits the lowest R^2 value in both scenarios. Conversely, the linear SVM (LSVM) and quadratic SVM (QGSVM) show the highest R^2 values. In terms of root-mean-square error (RMSE) values, the FGSVM has the highest value, while the LSVM has the lowest value.

Furthermore, the influence of VOD and CPBCM were examined, and their impacts are in Table 5. A positive value indicates the sensitivity of the included parameter to the model, while a negative indicates otherwise. Linear support vector machine had a 4% and 80% increase in R^2 and RMSE values. The fine Gaussian support vector machine had a -54% decrease in R^2 value, but the RMSE value improved by 94%. An improvement of 14% was observed in the medium Gaussian support vector machine but a 75% improvement in the R^2 and RMSE values, respectively. The coarse Gaussian support vector machine improved R^2 and RMSE by 3% and 65%, respectively. The respective parity plots for the SVM models are illustrated in Fig. 5a–e. During the training and testing stages, 10-fold cross-validation was engaged. The corresponding plots are indicated in Fig. 5. The predicted value is on the vertical axis, and the true response is on the horizontal axis.

From the parity plot, the fine Gaussian support vector machine is indicated in Fig. 5a. Figure 5b represents the linear support vector machine, Fig. 5c is the coarse Gaussian support vector machine, Fig. 5d is the medium Gaussian support vector machine, and Fig. 5e represents the quadratic Gaussian support vector machine respectively.

The results from the SVM models were then compared with the empirical models as shown in Table 6. Based on Eqs. (9) to (18), empirical predictions were made. Afterward, the result was then compared with the actual flyrock throw distance determined using ProAnalyst software. The R^2 and RMSE values were then determined as shown in Table 6.

4 Conclusions

The predictive capability of linear, quadratic, fine Gaussian, medium Gaussian, and coarse Gaussian quadratic support vector machines (LS-SVM, QGSVM FGSVM, MGSVM, and CGSV) have been examined.

The best-examined model for flyrock throw distance prediction is the linear support vector machine with R^2 and RMSE values of 1.00 and 0.05, respectively. The achieved result was better than those produced by empirical predictions.

The significant contribution offered by the inclusion of VOD and CPBCM was determined.

The magnitudes of improvement in R^2 an RMSE for the LS-SVM, FGSVM, MGSVM, CGSVM, and QGSVM are 0.00% and 80.00%, 39.5.00% and 94.00%, 14.00% and 75.00%, 3.00% and 65.00%, and then 1.00% and 98.00% respectively.

This work is limited to the Ghanaian mining environment but can be replicated elsewhere provided, and collected data has been trained and tested in the model applied.

Declarations

Ethical Statement The research is claimed to have been conducted following ethical guidelines

Conflict of Interest The authors declare no competing interests.

References

1. Lwin MM, Aung ZM (2019) Prediction and controlling of flyrock due to blasting for Kyaukpahto gold mine. Int J Adv Sci Res Eng 5(10):1–9, 338–346, Mandalay Myanmar. https://doi.org/10.31695/IJASRE.2019.33574

2. Hasanipanah M, Armaghani DJ, Amnieh HB, Abd Majid MZ, Tahir MM (2017) Application of PSO to develop a powerful equation for prediction of flyrock due to blasting. Neural Comput & Applic 28(1):1043–1050. https://doi.org/10.1007/s12665-016-6335-5

3. Shi JJ, An HM, Wu CP (2013) Analysis of the movement trajectory of blasting flyrock in the bottom of open pits. Advanced Mat Res 774:64–67. Trans Tech Publications Ltd. https://doi.org/10.4028/www.scientific.net/AMR

4. Kecojevic V, Radomsky M (2005) Flyrock phenomena and area security in blasting-related accidents. Saf Sci 43(9):739–750

5. Raina AK, Murthy VMSR, Soni AK (2014) Flyrock in bench blasting: a comprehensive review. Bull Eng Geol Environ 73(4):1199–1209

6. Mohamad ET, Yi CS, Murlidhar BR, Saad R (2018) Effect of geological structure on flyrock prediction in construction blasting. Geotech Geol Eng 36(4):2217–2235

7. Amini H, Gholami R, Monjezi M, Torabi SR, Zadhesh J (2011) Evaluation of flyrock phenomenon due to blasting operation by support vector machine. Neural Comput & Applic 21(8):1–9

8. Dindarloo SR (2015) Peak particle velocity prediction using support vector machines: a surface blasting case study. J S Afri Inst Min and Metall 115(7):637–643

9. Arthur CK, Temeng VA, Ziggah YY (2020) Multivariate adaptive regression splines (MARS) approach to blast-induced ground vibration prediction. Int J Min Reclam Environ 34(3):198–222

10. Arthur CK, Temeng VA, Ziggah YY (2020) Novel approach to predicting blast-induced ground vibration using Gaussian process regression. Eng Comput 36(1):29–42

11. Ye J, Koopialipoor M, Zhou J, Armaghani DJ, He X (2021) A novel combination of tree-based modeling and Monte Carlo simulation for assessing risk levels of flyrock induced by mine blasting. Nat Resour Res 30(1):225–243

12. Hasanipanah M, Faradonbeh RS, Armaghani DJ, Amnieh HB, Khandelwal M (2017) Development of a precise model for prediction of blast-induced flyrock using regression tree technique. Environ Earth Sci 76(1):1

13. Armaghani DJ, Momeni E, Abad SV, Khandelwal M (2015) Feasibility of ANFIS model for prediction of ground vibrations resulting from quarry blasting. Environ Earth Sci 74(4):2845–2860

14. Faradonbeh RS, Armaghani DJ, Monjezi M, Mohamad ET (2016) Genetic programming and gene expression programming for flyrock assessment due to mine blasting. Int J Rock Mechanics and MinSci 88:254–264

15. Asl PF, Monjezi M, Hamidi JK, Armaghani DJ (2018) Optimization of flyrock and rock fragmentation in the Tajareh limestone mine using metaheuristics method of firefly algorithm. Eng Comput 34(2):241–251

16. Khandelwal M, Monjezi M (2013) Prediction of flyrock in open pit blasting operation using machine learning method. Int J Min Sci Technol 23(3):313–316. https://doi.org/10.1016/j.ijmst

17. Monjezi M, Mehrdanesh A, Malek A, Khandelwal M (2013) Evaluation of effect of blast design parameters on flyrock using artificial neural networks. Neural Comput Applic 23(2):349–356

18. Monjezi M, Hasanipanah M, Khandelwal M (2013) Evaluation and prediction of blast-induced ground vibration at Shur River Dam, Iran, by artificial neural network. Neural Comput Applic 22(7):1637–1143

19. Monjezi M, Bahrami A, Varjani AY, Sayadi AR (2012) Prediction and controlling of flyrock in blasting operation using artificial neural network. Arab J Geosci 4(3-4):421–425

20. Yari M, Monjezi M, Bagherpour R, Sayadi AR (2015) Blasting operation management using mathematical methods. Eng Geol Soc Territory. Springer, Cham 1:483–493

21. Amini H, Gholami R, Monjezi M, Torabi SR, Zadhesh J (2012) Evaluation of flyrock phenomenon due to blasting operation by support vector machine. Neural Comput Applic 21(8):2077–2085

22. Armaghani DJ, Hajihassani M, Monjezi M, Mohamad ET, Marto A (2015) Blast-induced air and ground vibration prediction: a particle swarm optimization-based artificial neural network approach. Environ. Earth Sci 74(4):2799–2817

23. Khandelwal M, Singh TN (2011) Predicting elastic properties of schistose rocks from unconfined strength using intelligent approach. Arab J Geosci 4:435–442. https://doi.org/10.1007/s12517-009-0093-6

24. He Z, Armaghani DJ, Masoumnezhad M, Khandelwal M, Zhou J, Bhatawdekar RM (2021) A combination of expert-based system and advanced decision-tree algorithms to predict air-overpressure resulting from quarry blasting. Nat Resour Res 30:1889–1903. https://doi.org/10.1007/s11053-020-09773-6

25. Armaghani DJ, Hajihassani M, Mohamad ET, Marto A, Noorani SA (2014) Blasting-induced flyrock and ground vibration prediction through an expert artificial neural network based on particle swarm optimization. Arab J Geosci 7(12):5383–5396

26. Monjezi M, Bahrami A, Varjani AY (2010) Simultaneous prediction of fragmentation and flyrock in blasting operation using artificial neural networks. Int J Rock Mech Min Sci 47(3):476–480

27. Rezaei M, Monjezi M, Varjani AY (2011) Development of a fuzzy model to predict flyrock in surface mining. Saf Sci 49(2):298–305

28. Mohamad ET, Armaghani DJ, Hajihassani M, Faizi K, Marto A (2013) A simulation approach to predict blasting-induced flyrock and size of thrown rocks. Electron J Geotech Eng 18(B):365–374

29. Ghasemi E, Amini H, Ataei M, Khalokakaei R (2014) Application of artificial intelligence techniques for predicting the flyrock distance caused by blasting operation. Arab J Geosci 7(1):193–202

30. Marto A, Hajihassani M, Jahed Armaghani D, Tonnizam Mohamad E, Makhtar AM (2014) A novel approach for blast-induced flyrock prediction based on imperialist competitive algorithm and artificial neural network. Sci World J 2014(643715):11. https://doi.org/10.1155/2014/643715

31. Trivedi R, Singh TN, Raina AK (2014) Prediction of blast-induced flyrock in Indian limestone mines using neural networks. J Rock Mech Geotech Eng 6(5):447–454

32. Saghatforoush A, Monjezi M, Faradonbeh RS, Armaghani DJ (2016) Combination of neural network and ant colony optimization algorithms for prediction and optimization of flyrock and back-break induced by blasting. Eng Comput 32(2):255–266

33. Raina AK, Murthy VM, Soni AK (2015) Flyrock in surface mine blasting: understanding the basics to develop a predictive regime. Curr Sci 25:660–665

34. Sawmliana C, Hembram P, Singh RK, Banerjee S, Singh PK, Roy PP (2020) An investigation to assess the cause of accident due to flyrock in an opencast coal mine: a case study. J Inst Eng (India): Series D 101(1):15–26

35. Hasanipanah M, Amnieh HB (2020) A fuzzy rule-based approach to address uncertainty in risk assessment and prediction of blast-induced flyrock in a quarry. Nat Resour Res 29(2):669–689

36. Anon., (2020), "Goldfields Damang", www.goldfields.com/reports/rr_2008/int_damang.php, Accessed: May 30, 2020

37. Anon., (2011), "Mineral resource and mineral reserve overview - gold fields, technical report 2011", pp. (1-12), Accessed 4th April 2021, https://www.goldfields.com › reports › tech_damang.

38. Gunning DR, Whiting B (2009) Reserves and resources in the San Martín Mine, Mexico, as of July 31, 2009. For Starcore International Mines LTD, p 85

39. Mishra AK, Rout M (2011) Flyrocks–detection and mitigation at construction site in blasting operation. World Environ 1(1):1–5

40. Richards AJ, Moore AB (2005) Golden pike cut back fly rock control and calibration of a predictive model. Terrock Consulting Engineers Report, Kalgoorlie Consolidated Gold Mines, p 37

41. Chiapetta RF 1983. The use of high speed motion picture photography in blast evaluation and design. In Proceedings of the Ninth Conference on explosives and blasting technique-Soc Explosives Eng-Annual meeting, Jan. 31-Feb'4, 1983, Dallax, Taxas.

42. Lundborg N (1981) The probability of flyrock damages, vol 5. Swedish Detonic Research Foundation, Stockholm DS, p 39

43. Lundborg N, Persson A, Ladegaard-Pedersen A, Holmberg R (1975) Keeping the lid on flyrock in open-pit blasting. Eng Min J 176:95–100

44. Gupta RN (1980) Surface blasting and its impact on environment. In: Trivedi NJ, Singh BP (eds) Impact of mining on environment. Ashish Publishing House, New Delhi, pp 23–24

45. Awad, M. and Khanna, R. (2015), "Support vector machines for classification", www.researchgate.net/publication/300723807, https://doi.org/10.1007/978-1-4302-5990-9_3, pp. 28.

46. Vapnik VN (1999) An overview of statistical learning theory. IEEE Trans Neural Netw 10(5):988–999

47. Bordoloi DJ, Tiwari R (2014) Support vector machine based optimization of multi-fault classification of gears with evolutionary algorithms from time–frequency vibration data. Measurement. 55:1–4

48. Esmaeili M, Salimi A, Drebenstedt C, Abbaszadeh M, Bazzazi AA (2015) Application of PCA, SVR, and ANFIS for modeling of rock fragmentation. Arab J Geosci 8(9):6881–6893

49. Du J, Liu Y, Yu Y, Yan W (2017) A prediction of precipitation data based on support vector machine and particle swarm optimization (PSO-SVM) algorithms. Algorithms. 10(2):57

50. An S, Liu W, Venkatesh S (2007) Fast cross-validation algorithms for least squares support vector machine and kernel ridge regression. Pattern Recogn 40(8):2154–2162

51. Vapnik V (2013) The nature of statistical learning theory. Springer Science & Business Media

52. Bai J, Zhang XY, Duan JK 2008 Application of support vector machine with modified gaussian kernel in a noise-robust speech recognition system. In 2008 IEEE Int Symposium on Knowledge Acquisition and Modeling Workshop pp. 502-505.

53. Fischetti M (2016) Fast training of support vector machines with Gaussian kernel. Discret Optim 22:183–194

54. Evgeniou T, Pontil M (1999) Support vector machines: Theory Appl. In: Advanced Course on Artifl Intell. Springer, Berlin, Heidelberg, pp 249–257

55. McKenzie C (2018) "Flyrock model validation", ISEE 4th Annual Conference. Western Australia, Fremantle, pp 40